

MAGNETOTELLURIC OBSERVATIONAL TECHNIQUES ON LAND

GASTON FISCHER

Observatoire Cantonal, CH-2000 Neuchâtel, Switzerland

Abstract. During the period since the Workshops in Sopron and Murnau we have witnessed some quite remarkable changes in the techniques employed in magnetotelluric (MT) observations. These changes have brought about significant improvements in the quality of MT data that can be gathered today. The new techniques are very likely to bring improvements in many areas beside MT, but are reviewed here in the light of the progress they have rendered possible for MT soundings on land. Three main subjects are covered in this review. The first one is concerned with the use of cryogenic or SQUID magnetometers. The new instruments are presented to the geomagnetist. An explanation of how these instruments work is given without, however, details of their operation and fabrication, and without showing that they usually have a much larger, i.e. better, signal-to-noise ratio than conventional magnetometers. Next, the method of the remote magnetic reference is examined. Originally the MT method assumed incident signals in the form of plane waves. While it is known today that incident wave amplitudes which vary linearly with distance are perfectly acceptable for MT soundings, there are many other higher order distortions of the incident signal which are not acceptable. Most of these high order or local perturbations are man-made and can seriously falsify MT data. All processes of MT data analysis try to minimize the errors caused by locally perturbed signals. But they are only partly successful, especially when the perturbations produce strong cross-power bias. The remote magnetic reference method has proved far superior in avoiding most of this cross-power as well as faulty autopower. The last section of this review deals with the use in the field of microcomputers or microprocessors. These have made it possible to process the data on the site already to such a degree that the sounding crew knows whether the sounding is proceeding satisfactorily, and can decide how best to continue the survey work. Of particular interest is digital filtering, which is especially easy with the microcomputer, and which may be used to avoid specific sources of perturbation.

1. Introduction

During the past two or three years the techniques of magnetotelluric (MT) observation have evinced a number of significant improvements. As in other applications where electronics plays a dominant role, the emergence of the microcomputer, or microprocessor, has permitted great progress in both the speed and the complexity of data handling in the field. At the recent Working Group meeting in Canberra on Audio Electro-Magnetics (Vozoff, 1980b) the general feeling was that today one should not leave a site before a sounding has been successfully completed, or at least, one should know when leaving a site whether or not the sounding has been successful. To a large measure such a statement has only become possible because of the microcomputer. Significantly better MT data can also be gathered thanks to the use of a remote magnetic reference. In this new technique a sounding is carried out while the magnetic variations are recorded synchronously at a remote site, where the observed man-made perturbations are not correlated with those occurring at the sounding site itself. The last subject of this review concerns the use of SQUID magnetometers which can also markedly improve the quality of MT data that can be collected.

These three subjects were just emerging at the time of the Murnau Workshop and were briefly mentioned by Vozoff (1980a), whose review covered a very wide range of electromagnetic observational techniques. Here we plan to look at the three perhaps most important recent innovations related to the field of MT soundings in greater detail. It will become apparent, however, that the Berkeley MT group has been very active in all of these areas, and the present review ought perhaps to have been written by a member of this group. But at the end of April the Workshop organizers had little time left to look for the most appropriate speaker. As you can gather, the present review had to be put together in a rather short time.

We will be speaking first of a tool, the SQUID magnetometer; then of a technique, the method of external reference. Finally our attention will be directed toward data handling and managing, as we will be considering the microcomputer systems used right in the field.

2. The SQUID Magnetometer

Many detailed descriptions of SQUID devices have been published. We shall only mention a few of them here, often connected with their use as magnetometers (Clarke, 1973, 1977, 1979; Clarke *et al.*, 1976). The 1977 article by Clarke contains an extensive list of references to original work. The present review has been largely inspired by Solymar (1972), and Clarke (1977, 1979). Most presentations of SQUID magnetometers begin with the *dc* SQUID, which may be conceptually somewhat simpler. As commercially only *rf* SQUID systems seem to be available, we have chosen rather to present this latter type. But to get a detailed picture of the design problems and of the way SQUID magnetometers and other SQUID devices function, the reader is referred to the specialised literature (e.g., Solymar, 1972; Clarke *et al.*, 1976; Clarke, 1977), as the purpose of the present review is only to acquaint the geomagnetist with the basic principle of these magnetometers.

The SQUID magnetometer is a Superconducting QUantum Interference Device. It exhibits quantum properties at a macroscopic scale. Imagine a ring or hollow cylinder, as in Figure 1, composed of a superconducting metal like lead and being cooled below its superconducting temperature T_c . As it passes through T_c any weak magnetic field is excluded from the superconductor, except for a thin layer of thickness λ , the penetration depth. Typically λ is of the order of 50 nm. Inside and outside the hollow cylinder the field will persist (to avoid demagnetizing effects imagine that the cylinder axis is parallel to the field). To sustain the field-free region between inside and outside walls of the hollow cylinder, permanent currents must flow within the penetration depth of the cylinder wall. The mere existence of such non-dissipative permanent currents is already a quantum effect at the macroscopic scale of the cylinder dimensions. This current is therefore quantized and carried by the superconducting electron pairs of the metal. As a consequence the total flux inside the cylinder, integrated from the field-free region between the cylinder walls, is quantized too:

$$\phi_{\text{int}} = n\phi_0 = n\frac{h}{2e}, \quad (1)$$

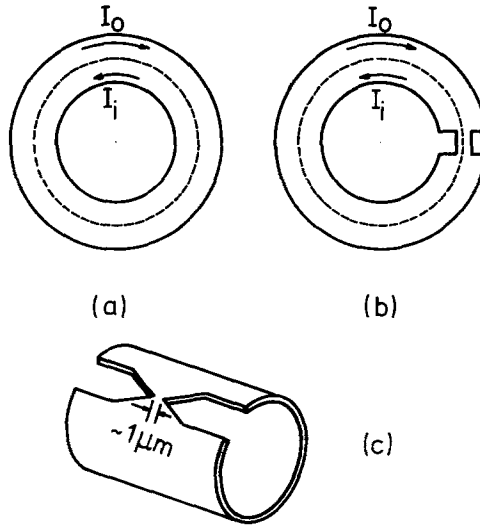


Fig. 1. (a) Superconducting cylinder in a magnetic field. The surface currents I_0 and I_i cancel any field inside the superconductor where the dashed contour of integration of Equation (3) can be placed. (b) Superconducting cylinder with a weak link or junction. (c) Practical geometry of an *rf* SQUID. Typically the cylinder diameter may be around 1 cm whereas the cylinder thickness could be 0.1 mm. But many other *rf* SQUID geometries are in common use.

where n is an integer, h is Planck's constant, and e is the electronic charge. The flux quantum

$$\phi_0 = 2.07 \times 10^{-15} \text{ Wb} = 2.07 \times 10^{-2} \text{ nT cm}^2 \tag{2}$$

appears to fall right into the range of parameters of interest to the geophysicist.

If the field applied to the cylinder of Figure 1a is varied, the current within the penetration depth of the outside wall will vary so as to continue cancelling the field inside the superconducting metal. Nothing of this change will be felt inside the cylinder. The two flux zones, inside and outside the cylinder, are therefore completely separated. The flux inside is a trapped flux; it cannot move out and no additional flux from outside can join it.

Equation (1) was obtained by specifying that the inside flux ϕ_{int} was calculated by integration over a surface bounded by a line placed everywhere deep inside the superconductor material. If we let this line come close to the inside wall of the hollow cylinder, the line will come into areas where currents flow, i.e., within a penetration depth of the inside wall. Some of the trapped flux will now lie outside the line and Equation (1) must be generalized to read

$$\phi_{\text{int}} + \mu_0 \oint \lambda^2 \mathbf{J} \cdot d\mathbf{s} = n\phi_0 \tag{3}$$

We assume now that the hollow cylinder is replaced by a cylinder with a weak link, as shown in Figures 1b and c. Because of the weak link it is no longer possible to claim that

the flux inside the cylinder is a trapped flux totally independent of the flux outside. Nor is it possible to place the line integral in Equation (3) in such a way that the second term on the left completely vanishes. In the area of the weak link this term will have to be finite, and flux will be able to move in and out of the cylinder precisely through that area. Even if we place as much as possible of the contour integral of Equation (3) in regions where the current disappears, we will be left with

$$\mu_0 \int_{\text{junction}} \lambda^2 \mathbf{J} \cdot d\mathbf{s} + \phi_{\text{int}} = n\phi_0. \quad (4)$$

Let us assume the junction to be really small, i.e., that the current in it is uniform. Let us also call I_i and I_o the currents that flow respectively on the inside and on the outside of the cylinder. We can then write approximately

$$J = (I_i - I_o)/A, \text{ uniform across junction}, \quad (5)$$

where A is the junction cross-section. If w is the junction length, Equation (4) can be written

$$\gamma L(I_i - I_o) + \phi_{\text{int}} = n\phi_0, \quad (6)$$

with

$$\gamma = \mu_0 \frac{\lambda^2 w}{AL}. \quad (7)$$

L is the inductance of the loop as seen from the current or voltage electrodes in Figure 2, or even more clearly from the following self-evident relation which connects the inside flux ϕ_{int} to the outside flux ϕ_{ext} :

$$\phi_{\text{int}} - \phi_{\text{ext}} = L(I_i - I_o). \quad (8)$$

Equations (6) and (8) can be combined to yield

$$\phi_{\text{int}} = \frac{1}{1+\gamma} (n\phi_0 + \gamma\phi_{\text{ext}}), \quad (9)$$

or

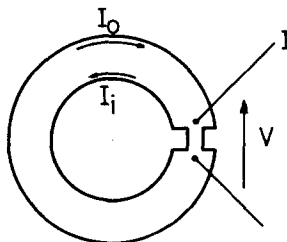


Fig. 2. Weakly connected ring with current or voltage electrodes at the junction.

$$LI_{\text{circ}} = L(I_i - I_0) = \frac{1}{1+\gamma} (n\phi_0 - \phi_{\text{ext}}). \quad (10)$$

Equation (10) tells us that when $\phi_{\text{ext}} = n\phi_0$ no current flows through the junction, i.e., that $I_{\text{circ}} = I_i - I_0 = 0$. When ϕ_{ext} increases or decreases a net current I_{circ} begins to flow through the junction. Because of the small dimensions of the junction this current soon reaches a critical value I_c , at which the junction may become normal:

$$(\phi_{\text{ext}})_c = n\phi_0 + (1 + \gamma) LI_c. \quad (11)$$

At this point the junction either turns normal (it only does so momentarily and returns to the superconducting state but with another quantum number n), for it is not capable of carrying such a large supercurrent, or it adjusts to another value of n without passing through a normal phase. To find out which of these alternatives will in fact occur we combine Equation (10), written for $(\phi_{\text{ext}})_c$ with $n+1$, and Equation (11),

$$LI_{\text{circ}} = L(I_i - I_0) = \frac{\phi_0}{1+\gamma} - LI_c. \quad (12)$$

Let us now introduce a new parameter α by the relation

$$I_c = \alpha \frac{\phi_0}{2(1+\gamma)L}. \quad (13)$$

With this parameter Equation (12) becomes

$$LI_{\text{circ}} = L(I_i - I_0) = \frac{2-\alpha}{\alpha} LI_c. \quad (14)$$

It is clear, then, that if

$$LI_{\text{circ}} = L(I_i - I_0) < LI_c \quad (15)$$

the transition to the state $n+1$ is possible and will indeed occur before the junction turns normal. If however,

$$LI_{\text{circ}} = L(I_i - I_0) > LI_c, \quad (16)$$

the junction turns normal before it can adjust to a new quantum number. The boundary between these two cases is at $(2-\alpha)/\alpha = 1$, i.e. at $\alpha = 1$, and we see in Figure 3 how the three situations $\alpha < 1$, $\alpha = 1$, and $\alpha > 1$ differ.

So far we have looked at the cylinder and its weak link from a dc point of view only. As long as the junction current remains below I_c no voltage appears across the junction. With ac currents, however, the situation is different, an ac voltage develops across the junction because of the self-inductance L , and because at ac there is a small absorption of energy even by a superconductor. The equivalent SQUID configuration becomes as shown in Figure 4, and the SQUID can then be used as a null detector in a flux-locked loop as sketched schematically in Figure 5. From what we have seen, the SQUID itself

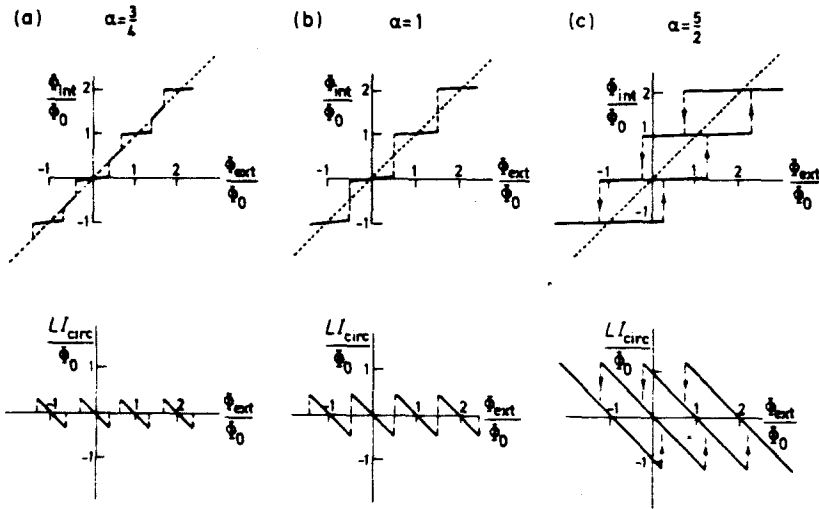


Fig. 3. Internal magnetic flux (Equation (9)) and circulating current (Equation (10)) of a weakly connected ring as a function of the external flux for (a) $\alpha = 3/4$, (b) $\alpha = 1$, and (c) $\alpha = 5/2$, where α is defined by Equation (13) (after Silver and Zimmerman, 1967).

is a strikingly non-linear device. As a result the *af* (audio-frequency) modulated *rf* oscillations, after detection of the *rf*, arrive at the input to the lock-in as a superposition of the fundamental *af* frequency f and several harmonics, especially the second harmonic $2f$. For a given reference field, and depending on the *rf* level, the signal at frequency f actually vanishes. Any departure from the reference field produces a signal at frequency f which is detected by the lock-in and integrated. This integrated signal is suitably fed back to the SQUID so as to reduce the signal at f . The output is therefore highly proportional to the departure from the initial reference field and the SQUID in the flux-locked loop arrangement becomes an eminently linear magnetometer. In practice the SQUID is usually operated at $n = 0$, or at a low value of n . In a null detector arrangement, as in Figure 5, the flux inside the SQUID remains constant. To isolate the SQUID from all external field variations, it is mounted inside a superconducting shield. Changes of the quantum number n correspond to so-called flux jumps. Such jumps can occur if the electronics is incapable of following a rapid field change. This will happen more frequently the higher the system sensitivity. The main advantage of the SQUID over other magnetometers is its low noise. But a detailed evaluation of SQUID noise is beyond the scope of this review, especially as this subject is abundantly covered in the literature we have quoted at the

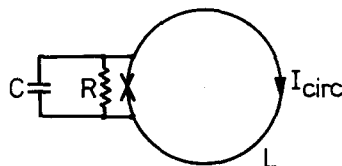


Fig. 4. Equivalent circuit of an *rf* SQUID subjected to an *ac* excitation.

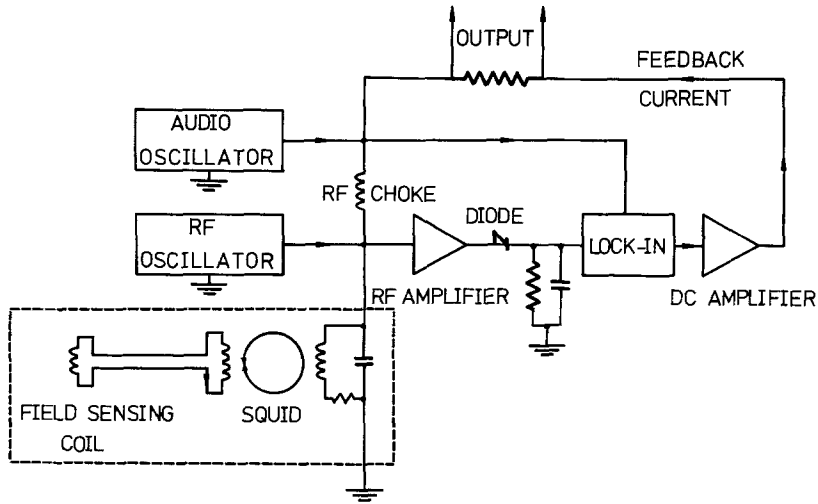


Fig. 5. Simplified circuitry of an *rf* SQUID magnetometer in a flux-locked loop. The elements within the dashed line are at liquid helium temperature. The SQUID and the two adjacent coils are inside a superconducting shield to insure their isolation from all external influences (partly after Clarke, 1973, 1977).

beginning of this section. This completes our description of the *rf* SQUID magnetometer.

The *dc* SQUID is quite similar, but it comprises two junctions and one can show that the two weakly-coupled superconductors may acquire different *dc* potentials. The detection is in terms of that *dc* potential and no *rf* is necessary. In other respects the operation of the *dc* SQUID is almost the same as that of the *rf* SQUID, and similar performances can be achieved. Today the most sensitive *dc* SQUID probably surpasses the *rf* SQUID (Voss *et al.*, 1980; Clarke, 1980).

3. The Use of SQUID Magnetometers

We have seen in the preceding section that SQUID magnetometers directly measure the field and not its rate of change with time. In addition, the commercially available instruments have properties which equal or surpass the following list.

- (1) Noise figures of 10^{-5} or 10^{-6} nT Hz^{-1/2}.
- (2) Flat responses from 10^4 or 10^5 Hz to *dc*.
- (3) Dynamic ranges in excess of 160 dB.

In this respect it should be noted that point (1) depends essentially on the SQUID design, whereas (2) and (3) are generally given by the associated electronics. Voss *et al.* (1980) have recently designed *dc* SQUIDS with much lower noise figures. It may also be worth pointing out that today's superinsulated liquid helium dewars have become more compact and are less delicate to handle than the dewars of ten years ago. For example a liquid nitrogen envelope is no longer required. Liquid helium consumption is of the order of a litre per day. Depending on the desired period range, dewar capacities between 1 and 30 l

have been used. Motion noise of SQUID systems can be a delicate problem. Proper mounting of the SQUID inside the dewar is essential, as well of course as stable positioning of the dewar in the field.

The first reported use of SQUID magnetometers in geomagnetic measurements is probably by Buxton and Fraser-Smith (1974), who looked at PC-1 pulsations both with an *rf* SQUID and with a good standard magnetometer. A significant improvement of signal-to-noise could already be reported, as is evident from Figure 6 obtained with a system $S/N = 3 \times 10^{-5} \text{ nT Hz}^{-1/2}$. Clarke *et al.* (1978) then performed MT soundings with two triple axis SQUIDs. As a matter of fact the Berkeley group (Gamble *et al.*, 1979a, b) carried out simultaneous soundings with *dc* and *rf* SQUIDs to study and demonstrate the remote magnetic reference method which will be described in the following section. The data of Figure 7 were obtained with a *dc* SQUID ($S/N = 10^{-5} \text{ nT Hz}^{-1/2}$) whereas the Figure 8 data have been obtained with a commercial *rf* SQUID ($S/N = 10^{-4} \text{ nT Hz}^{-1/2}$). The Figures 7 and 8 data cannot be compared with data obtained by standard means. As will be seen later they exhibit very little scatter because of the use of a remote magnetic reference. Of greater significance, in our view, is the wide period range of practically four decades achieved by this system, and the limitations are not due to the SQUIDs, but are given by the electronics. To compare SQUID performances with those of standard systems it is better to look at the earlier data of Buxton and Fraser-Smith (1974). Figure 6 makes it quite clear that the noise level of the SQUID system is significantly lower than that of the classical system, in spite of an evidently wider frequency response. Natural spikes in the spectrum come out far more sharply with the SQUID than with the standard system.

SQUID magnetometers have been used successfully for several years in commercially available rock-magnetometers. Their deployment in MT work is more recent, with perhaps the first report by the USGS (cf. Stanley *et al.*, 1977). Now even commercial firms advertise MT soundings with cryogenic magnetometers.

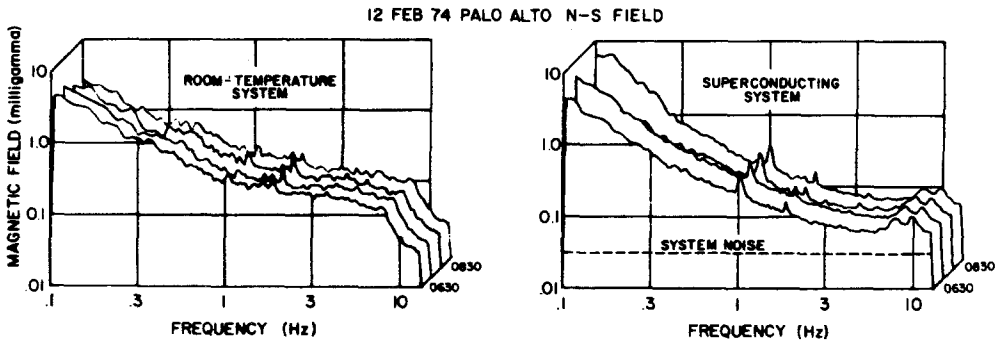


Fig. 6. Comparison of a superconducting *rf* SQUID system with a good conventional system. The spectra were taken simultaneously. In the region above 1 Hz, the natural spectrum drops well below the 0.1 pT (picoTesla) line. Also evident is the limited frequency response of the conventional system (after Buxton and Fraser-Smith, 1974). The spikes at one Hz are calibration marks.

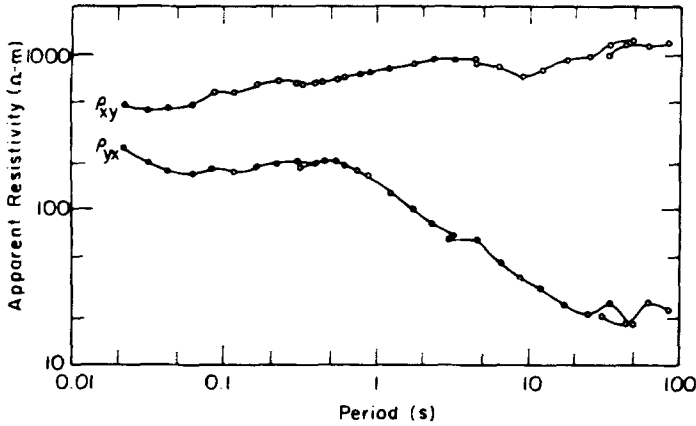


Fig. 7. Apparent resistivities obtained at Upper La Gloria with a tri-axial *rf* SQUID system. The remote magnetic reference method was used to obtain these data. The reference field was recorded at Lower La Gloria with *dc* SQUIDS (after Gamble *et al.*, 1979).

4. Magnetotellurics with a Remote Magnetic Reference

After completing a sounding the next step is the determination of the impedance coefficients $Z_{ik}(T)$ as a function of the period T . These coefficients are defined by the relations

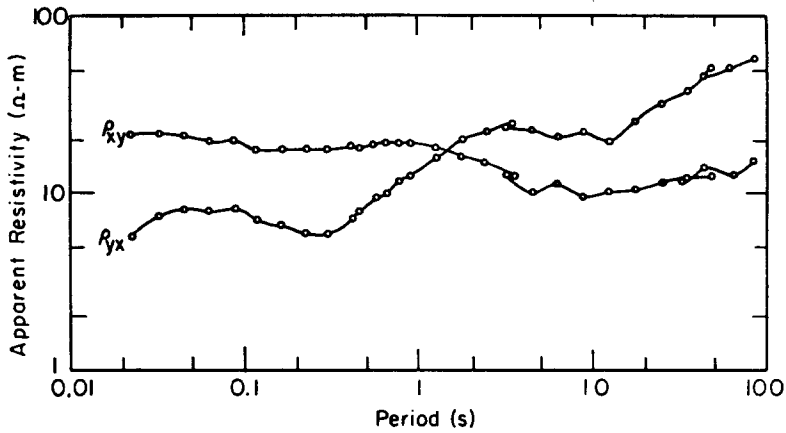
$$E_x(T) = Z_{xx}(T)H_x(T) + Z_{xy}(T)H_y(T) , \tag{17}$$

$$E_y(T) = Z_{yx}(T)H_x(T) + Z_{yy}(T)H_y(T) .$$

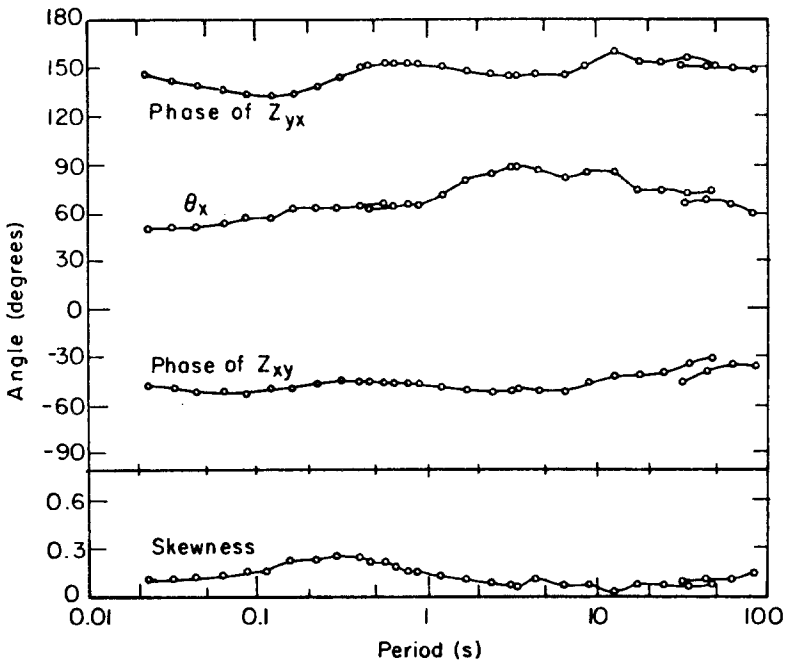
Because the incoming signals do not always satisfy the requirement that they be equivalent to plane waves (although it is known today that incident waves with linearly varying amplitudes still lead to the correct impedance (cf. Dimitriev and Berdichevsky, 1979; Schmucker, 1980)), and because of noise sources in the electronics itself, the determination of the $Z_{ik}(T)$ is a statistical problem. How this problem might be tackled has been described in detail by Sims and Bostick (1969) and Sims *et al.* (1971), whose method is probably still the most widely used. These authors have shown that each tensor coefficient $Z_{ik}(T)$ can be expressed in four different stable ways, two of which in general overestimate the impedance modulus, while the other two in general underestimate it. For the sake of our discussion we give one each of these two groups of estimates,

$$Z_{xy} = \frac{\langle E_x E_x^* \rangle \langle E_y^* H_x \rangle - \langle E_x E_y^* \rangle \langle E_x^* H_x \rangle}{\langle E_x^* H_y \rangle \langle E_y^* H_x \rangle - \langle E_x^* H_x \rangle \langle E_y^* H_y \rangle} , \tag{18}$$

$$Z_{xy} = \frac{\langle E_x H_y^* \rangle \langle E_y^* H_x \rangle - \langle E_x E_y^* \rangle \langle H_x H_y^* \rangle}{\langle H_y H_y^* \rangle \langle E_y^* H_x \rangle - \langle H_x H_y^* \rangle \langle E_y^* H_y \rangle} . \tag{19}$$



(a)



(b)

Fig. 8. Apparent resistivities (a), as well as phases, orientation angle and skewness (b) obtained at Lower La Gloria with a tri-axial *dc* SQUID system. The remote magnetic reference method was used to obtain these data. The reference field was recorded at Upper La Gloria with *rf* SQUIDs (after Gamble *et al.*, 1979).

The symbols $\langle \rangle$ mean averages over the N samples available, although this summation is sometimes also carried out over several neighbouring periods,

$$\langle E_x H_y^* \rangle = \sum_{i=1}^N E_{xi}(T) H_{yi}^*(T). \quad (20)$$

Before the advent of the powerful FFT algorithm, the computation of $E_{xi}(T) H_{yi}^*(T)$ was often done by the method of cross-power spectra (auto-power for products like $E_{xi}(T) E_{xi}^*(T)$),

$$E_{xi}(T) H_{yi}^*(T) = \frac{1}{M^2} \sum_{k=1}^M \left[\sum_{h=1}^M E_{xi}(h\delta) H_{yi}^*((h-k)\delta) \right] e^{i2\pi nmk\delta}, \quad (21)$$

where δ is the sampling interval, $M\delta$ the sample length (the samples are usually windowed, so that for $h < 1$ and $h > M$ they vanish), and $nv = n/M\delta = 1/T$ is the inverse period.

In the absence of perturbing cross-power and if the structure is one-dimensional, the two ratios (18) and (19) reduce to the well-known simple forms

$$Z_{xy} = \frac{\langle E_x E_x^* \rangle}{\langle E_x^* H_y \rangle}, \quad (22)$$

$$Z_{xy} = \frac{\langle E_x H_y^* \rangle}{\langle H_y H_y^* \rangle}, \quad (23)$$

which exemplify the tendency for Equation (18) to overestimate the modulus of $Z_{xy}(T)$, and for Equation (19) to underestimate this modulus when there is faulty auto-power.

Looking at Equations (18) to (23) one is tempted to conclude that the impedances $Z_{ik}(T)$ are particularly sensitive to perturbations which affect the auto-power estimates. This observation led Kao and Rankin (1977) to propose an iterative procedure to eliminate the auto-powers. Their technique brought a significant improvement of data which were biased essentially by faulty auto-powers, but was ineffective when there was bias in the cross-powers as well. Goubau *et al.* (1978) then succeeded in deriving the analytical equivalent of the Kao and Rankin (1977) procedure and confirmed that it improves data that are not too dispersed to begin with, but increases the scatter of the poor data.

Working on the idea of reducing the noise in both auto-power and cross-power spectra, Gamble *et al.*, (1979a, b) then proposed the method of remote magnetic reference, which was immediately looked upon as a big step forward. The basic idea of this method is that source signals which do not satisfy the criteria of an incoming plane wave produce effects which are quite local and are, therefore, not correlated with signals observed at a distant station. If the sounding site and the reference site were both on tabular or 1-D structures, the unperturbed parts of the magnetic signals would be almost identical at both sites; the cross-powers due to these signals would be very large indeed, and at the same time the

uncorrelated perturbations would not be able to bias these power estimates. When the two sites are not on tabular structures the cross-powers will be somewhat reduced, but since the noise-power remains small the impedance estimates remain good. The essential requirements for the remote reference method to be applicable are therefore twofold: there must be a linear relationship between the unperturbed signals at the measurement and reference sites, this will insure an important contribution to the unperturbed cross-power; simultaneously, however, the perturbations at the two sites must be as little correlated as possible to avoid the generation of perturbed cross-power. Furthermore, as can be deduced by considering an equation like (21), the unperturbed cross-power will be larger if the two sites are similar, but the determining factor is the ratio of perturbed to unperturbed cross-power. If we call $H_{xr}(T)$ and $H_{yr}(T)$ the magnetic field at the reference site, then as shown by Gamble *et al.* (1979a),

$$\begin{aligned}
 Z_{xx} &= [\langle E_x H_{xr}^* \rangle \underline{\langle H_y H_{yr}^* \rangle} - \underline{\langle E_x H_{yr}^* \rangle} \langle H_y H_{xr}^* \rangle] / D \\
 Z_{xy} &= [\underline{\langle E_x H_{yr}^* \rangle} \underline{\langle H_x H_{xr}^* \rangle} - \langle E_x H_{xr}^* \rangle \langle H_x H_{yr}^* \rangle] / D \\
 Z_{yx} &= [\underline{\langle E_y H_{xr}^* \rangle} \underline{\langle H_y H_{yr}^* \rangle} - \langle E_y H_{yr}^* \rangle \langle H_y H_{xr}^* \rangle] / D \\
 Z_{yy} &= [\underline{\langle E_y H_{yr}^* \rangle} \underline{\langle H_x H_{xr}^* \rangle} - \underline{\langle E_y H_{xr}^* \rangle} \langle H_x H_{yr}^* \rangle] / D
 \end{aligned} \tag{24}$$

where

$$D = \underline{\langle H_x H_{xr}^* \rangle} \underline{\langle H_y H_{yr}^* \rangle} - \langle H_x H_{yr}^* \rangle \langle H_y H_{xr}^* \rangle .$$

In these equations it is easy to distinguish the underlined first order from second order power estimates.

To illustrate what can be achieved by the remote reference method we show some results obtained by Gamble *et al.* (1979a, b) at the Upper and Lower La Gloria sites. These two sites are separated by about 5 km. They were operated simultaneously, synchronization being achieved by a telemetry link. The magnetic field at one station served as remote reference for the other, and vice-versa. We see in Figures 9 and 10 the results obtained at Upper La Gloria by the standard methods and in Figures 7 and 8 data derived from the remote reference technique. It is quite clear that the new method leads to a marked improvement of the data, especially when the coherency between measured and predicted electric field is below about 0.9, and the standard data are obviously very bad.

Elsner *et al.* (1982) have also carried out MT measurements with a remote magnetic reference station in Germany. With a remote station essentially free from perturbations they attempt to study what sort of interferences affect standard soundings and what effect these interferences have on the results.

Schnegg *et al.* (1980) looked at the improvements possible at AMT (audio-frequency MT) with a remote magnetic reference. Instead of using a telemetry link between the two

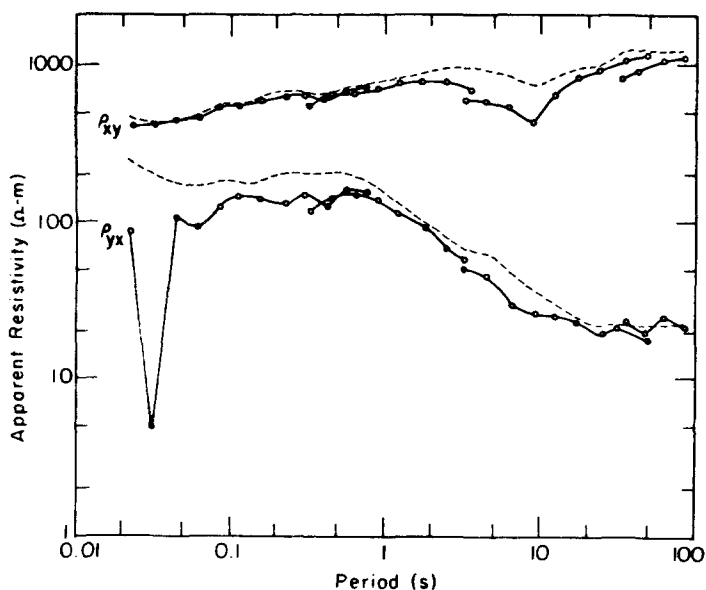


Fig. 9. Apparent resistivities versus period obtained at Upper La Gloria with a tri-axial *rf* SQUID system. These data were computed with a method that generally underestimates the modulus of the impedance and consequently also the apparent resistivity (after Gamble *et al.*, 1979).

stations they synchronized their two stations with the HBG timing signal. There are many transmitters of such timing signals in Europe, and at least one in North America, which can be used for these purposes (cf. Bonanomi and Schumacher 1976a, b; Schumacher 1979; Bonanomi 1979). Schnegg *et al.* (1980) concluded that the remote magnetic reference does not, in general, bring much improvement to the quality of AMT data, at

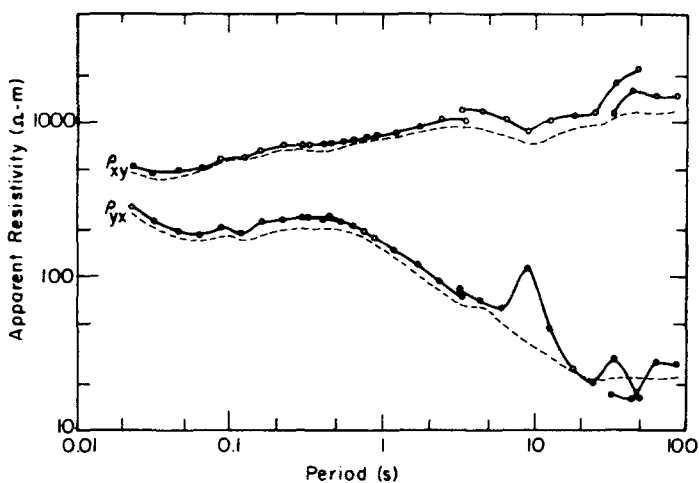


Fig. 10. Apparent resistivities versus period obtained at Upper La Gloria with a tri-axial *rf* SQUID system. These data were computed with a method that generally overestimates the modulus of the impedance and consequently also the apparent resistivity (after Gamble *et al.*, 1979).

least not in highly perturbed areas of western Europe, because the observed perturbation amplitudes are usually much higher than the natural signal amplitudes. In fact, the data are even degraded when the reference site is more perturbed than the measurement site. As a first tool against the strong man-made disturbances Schnegg *et al.* (1980) propose the delay-line filtering technique, which will be discussed in the next section. This technique has been shown to bring significant improvements to AMT data (Schnegg and Fischer 1979a, b, 1980).

It is worth, at this point, mentioning a method somewhat related to that of the remote magnetic reference. This is the telluric-magnetotelluric method utilized by the Brown University group (Hermance and Thayer 1975; Hermance *et al.*, 1976; Thayer *et al.*, 1981). Here a complete MT base station is operated, as well as several remote or satellite telluric stations. At the base station the local impedance tensor $[Z^b]$ is obtained. With simultaneous electric measurements one can get a telluric transfer tensor $[T]$, connecting the remote field \mathbf{E}^r to the base field \mathbf{E}^b ,

$$\mathbf{E}^r = [T] \mathbf{E}^b . \quad (25)$$

Note that no magnetic measurements are necessary to get $[T]$. If the two sites were tabular, the magnetic field would be essentially the same at the two sites, $\mathbf{H}^r \approx \mathbf{H}^b$, and the impedance at the remote site would then be given by

$$[Z^r] \approx [T] [Z^b] . \quad (26)$$

In general, however, one does not have

$$\mathbf{H}^r \approx \mathbf{H}^b \quad (27)$$

and the approximate Equation (26) does not hold, although Hermance and Thayer (1975) have reported agreements within 10% between the correct $[Z^r]$ and the one inferred from the approximate relation (26) for a variety of sites in Iceland. The main point to be made, however, is that Equation (25) relates observations at distant sites. As a consequence local perturbations will not be correlated between the two sites and will not affect the determination of the telluric transfer tensor $[T]$, the scattering range of which should be quite small. If the base station is a good site, then $[Z^b]$ can be determined with accuracy and the scatter in the approximate $[Z^r]$ given through relation (26) will be small too. Except for the fact that relation (26) is at best an approximation, the telluric-magnetotelluric technique does, however, embody some of the interesting features of the remote magnetic reference method: uncorrelated noise at the two sites does not, in general, perturb the determination of the transfer tensor $[T]$.

5. The Microcomputer and Data Management in the Field

As has been said in the introduction, the microprocessor or microcomputer has, in a sense, revolutionized the management of MT data in the field, often giving the measuring crew

sufficient information about the sounding in progress to allow them to decide about the future course of action. Where microprocessors are employed real progress has had to await the arrival of the 16 bit unit to handle the necessary dynamic range. With computers the only limitation concerns power consumption.

The first extensive use of a microprocessor to handle all data in the field and immediately perform a series of extensive computations to give preliminary results about the site has probably been reported by Schnegg and Fischer (1979a, b; 1980). Their microprocessor is a TM 990 and uses a very efficient FFT over 240 points based on an algorithm by Winograd (cf. Silverman, 1977). In connection with their AMT equipment (1–1000 Hz) the system can display on a scope the spectra of any of the five measuring channels. While a sounding is in progress, gradually improving apparent resistivities, $\rho_{xy}(T)$ or $\rho_{yx}(T)$, or the corresponding phases, $\varphi_{xy}(T)$ or $\varphi_{yx}(T)$, can be displayed. The data is continuously checked for such things as amplifier overload and coherency, and rejected if certain criteria are not met. Additionally the system can perform rotations of the coordinate system, for example to the principal coordinates, or if the data appear to satisfy the 1-D criteria, the 1-D dispersion relations can be applied (Weidelt, 1972; Fischer and Schnegg, 1980) or a 1-D inversion carried out (Fischer, 1980, Fischer *et al.*, 1981). Similar systems built around a Digital Equipment Corp. LSI-11/03 microcomputer have recently been reported by the Berkeley group (Clarke *et al.*, 1980) and the Edinburgh group (Dawes, 1980). Other computer-controlled data acquisition systems have been mentioned, e.g., by Stanley *et al.*, (1977) and by Losecke *et al.* (1978, 1979).

These new systems of course produce digital records of the samples and it is thus easy to subject the data to digital filtering. This is especially important in the AMT range where the electric mains are responsible for strong perturbations at 50 or 60 Hz and their odd harmonics. In some countries, like Switzerland and Germany, the trains operate at $16\frac{2}{3}$ Hz and that fundamental frequency and its odd harmonics are also the source of strong perturbations. While these perturbations are by no means stationary, Schnegg and Fischer (1979a, b, 1980) observed that compared to the length of the fundamental periods, i.e., 60 ms for the trains and 20 ms for the mains, the perturbations were remarkably stable. This observation suggested that delay-line filters might be especially well suited to remove the perturbations, and this could be performed quite easily with the microprocessor. Suppose the signal in one of the channels is $g(t)$:

$$g(t) = \frac{1}{2\pi} \int d\omega G(\omega) e^{-i\omega t} \quad (28)$$

Since the samples are always of finite length there will generally be a window $w(t)$:

$$w(t) = \frac{1}{2\pi} \int d\omega W(\omega) e^{-i\omega t} \quad (29)$$

so that the samples signal is effectively $w(t) \cdot g(t)$. The spectrum of this product is a convolution of the two spectra $G(\omega)$ and $W(\omega)$. Suppose, however, that we use a delay-line filter, such that the filtered signal we store and process becomes

$$w(t) [g(t) - g(t - \delta)] \quad (30)$$

Assuming that $w(t)$ is symmetrical (an excellent review of the properties and the effects of various kinds of windows has recently been published by Harris (1978); any user of windows should be aware of that paper); it can be shown that the spectrum of the above filtered signal is given by

$$G_{w\delta}(\omega) = \frac{1}{2\pi} \int d\omega' \underbrace{G(\omega')}_{\text{signal}} \underbrace{[1 - e^{-i\omega'\delta}]}_{\text{delay-line}} \underbrace{W(\omega' - \omega)}_{\text{window}} \quad (31)$$

As one can see from this equation, if there is a true line-spectrum in the original signal at any frequency f_n such that

$$\omega'\delta = 2\pi f_n \delta = 2\pi n, \quad (32)$$

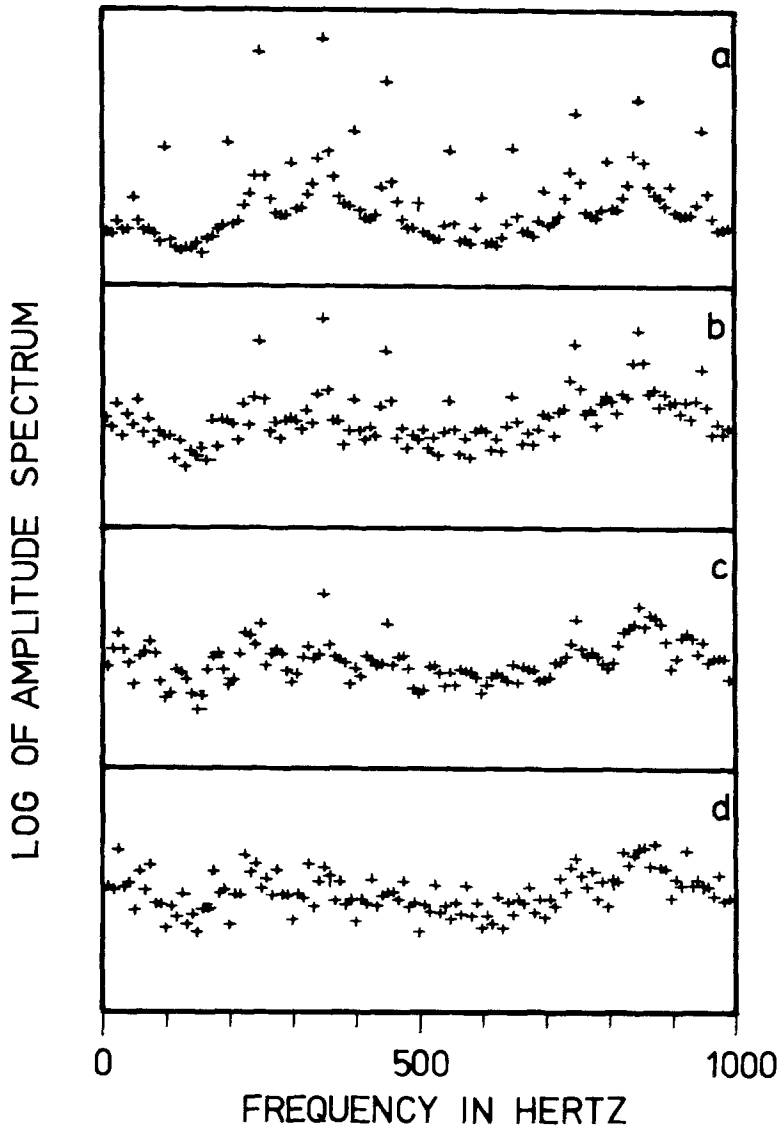
i.e., $f_n = \frac{n}{\delta}, \quad n = 0, 1, 2, 3, \dots,$

this line will not spoil the filtered signal. If we choose $\delta = 60$ ms, we get rid of any line at the $16\frac{2}{3}$ Hz from the trains and all their harmonics, including, e.g., the 50 Hz mains. In practice, however, these lines are not perfectly narrow, as this would mean that the perturbations are perfectly stationary. The lines can be reasonably broad if the perturbations change quickly, but how effective the filter actually is can be seen in Figure 11. Looking at Equation (31) we note that among the frequencies rejected from $G(\omega')$ we find the very low frequencies. The subtraction filter described by Equation (30) is therefore also a 'high-pass' filter. Furthermore, it can be shown, if one assumes that $g(t)$ and $g(t - \delta)$ are uncorrelated, that the power contained in the filtered signal is about twice the white noise power of the original signal.

Figure 11 illustrates the effect of the delay-line filters on the Fourier spectrum of an MT signal, here a telluric component on a somewhat resistive site. Trace (a) is obtained with no delay-line filter. Trace (b) results when a filter with $\delta = 60$ ms is inserted. We note that at high frequencies the filter appears to become ineffective. This arises because of the flutter of the analog tape from which this signal is taken. The flutter produces a frequency modulation of the signal and thus a broadening of the lines, especially at the higher frequencies. This effect would disappear completely with a real-time signal. Trace (c) is obtained with a filter where $\delta = 20$ ms and trace (d) arises when the two filters are used simultaneously.

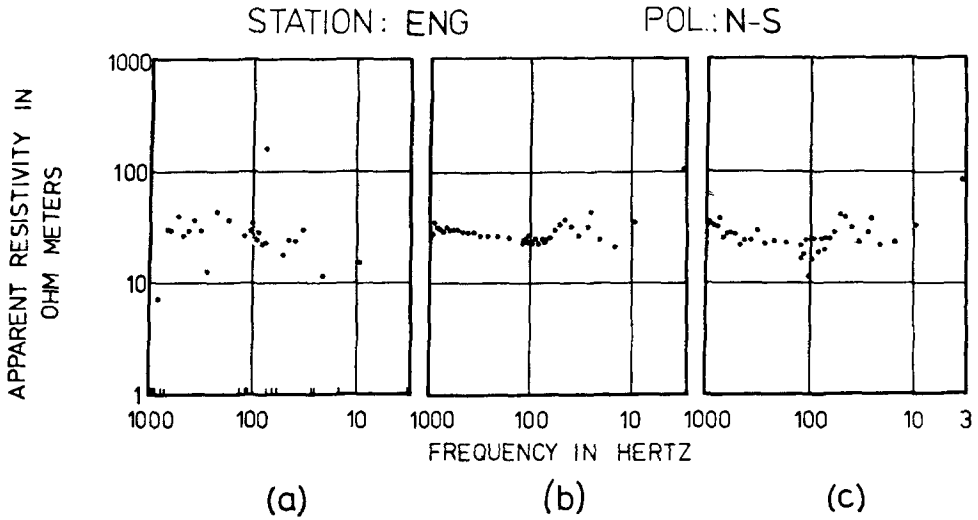
In Figure 12 we show three scope pictures obtained while a sounding is in progress. Picture (a) is displayed after 8 s (one cycle of sampling and processing). The lines at the bottom of the picture correspond to frequencies for which the data did not meet the minimum coherency criterion imposed. Picture (b) shows the situation after 13 min (96 cycles). Picture (c) is obtained in the same manner as (b), but without delay-line filter. An important distortion at 50 Hz is reduced, but a strong line at 25 Hz is left unfiltered.

A microprocessor can perform similar tasks of data handling and processing in the MT range, i.e., at the long periods, as for example in our 0.25–3000 s band. Here we use an



Delay line periodic filtering of MT data

Fig. 11. Fourier spectrum of a digitized electric signal. Trace (a) is obtained with no delay-line filter. Trace (b) results when a delay-line filter with $\delta = 60$ ms is inserted, and trace (c) when $\delta = 20$ ms. Trace (d) arises when the two filters are used simultaneously. Note that the original signal was first recorded on an analog tape and the very strong lines at $16\frac{2}{3}$, 50 and 150 Hz had already been partly removed with notch filters.



Oscilloscope display of an on-line AMT sounding

Fig. 12. Scope display of $\rho_{xy}(T)$ in the field at Engollon, where very little 16 2/3 Hz perturbation was felt. Picture (a) shows the situation with delay-line filters after 8 s, i.e., after one cycle of sampling and processing. The lines along the bottom trace correspond to frequencies at which the data did not meet the imposed coherency criterion. Picture (b) is displayed after about 13 min, with 96 data samples. Picture (c) is obtained in similar manner as (b), but without delay-line filtering. We note that the scatter in (b) is much smaller than in (c), that the 50 Hz perturbation has been reduced, but that a strong sub-harmonic at 25 Hz is unfortunately left untouched. The 25 Hz distortion is probably caused by motors working at or close to 1500 rpm.

additive delay-line filter,

$$g(t) + g(t + \delta) \tag{33}$$

which will eliminate all frequencies f_m such that

$$f_m = \frac{2m + 1}{2\delta} , \quad m = 0, 1, 2, \dots \tag{34}$$

Obviously we have here a 'low-pass' filter which can eliminate a fundamental frequency and all its odd harmonics.

In conclusion it can be said that the use of a microprocessor can greatly increase the flexibility of MT sounding equipment, without noticeably increasing its weight or power requirement. This is true not only at the high AMT frequencies, but also at much lower frequencies. The most important gain is the dialog it permits between the operator and the measurement. In addition all problems of automation, such as monitoring of signal level or quality, can be handled with very simple logistic means.

Summary

This review has dealt in some details with three recent technological developments in MT observational techniques. The SQUID magnetometers were considered first. Their main interest centers on their low noise figure, their flat frequency response, and their wide dynamic range. The remote magnetic reference method was considered next. It too should help in reducing the incidence of man-made noise on the data. Finally, the computer or microprocessor handling of data in the field will make this acquisition process much more efficient. The gains can be in speed, signal monitoring, dynamic range through digitization, noise reduction by digital filtering, and display of preliminary results on the sounding site.

Acknowledgements

The author gratefully acknowledges the help received from Drs P. Martinoli and J. Clarke. Financial support was provided by the Swiss National Science Foundation and the Geophysical Commission of the Swiss Academy of Natural Sciences.

References

- Bonanomi, J.: 1979, 'Horloges Asservies par Signaux Horaires', *Proc. Tenth Int. Congr. of Chronometry* 2, 97–103.
- Bonanomi, J. and Schumacher, P.: 1976a, 'Synchronisation d'Horloges par Signaux Horaires', *La Suisse Horlogère* 11–76, 229–235.
- Bonanomi, J. and Schumacher, P.: 1976b, *Quartz Clocks Synchronized by LF Time Signals*, Proc. Eighth Annual Precise Time and Time Interval (PTTI) Applications and Planning Meeting, Washington, 135–146.
- Buxton, J. L. and Fraser-Smith, A. C.: 1974, 'A Superconducting System for High Sensitivity Measurements of PC 1 Geomagnetic Pulsations', *IEEE Trans. Geosc. Electronics* GE-12, 109–113.
- Clarke, J.: 1973, 'Low-Frequency Applications of Superconducting Quantum Interference Devices', *Proc. IEEE* 61, 8–19.
- Clarke, J.: 1977, 'Superconducting Quantum Interference Devices for Low Frequency Measurements', in Schwartz, B. B. and Foner, S. (eds.), *Superconductor Applications: Solids and Machines*, Plenum Publ. Corp., New York, Chapter 3, pp. 67–124.
- Clarke, J.: 1979, 'Josephson Effect Devices', *Phys. Bull.* 30, 206–208.
- Clarke, J.: 1980, 'Advances in SQUID Magnetometers', *IEEE Trans. Electron. Devices* E-D-27, 1896–1908.
- Clarke, J., Gamble, T. D., Goldstein, N., Goubau, W. M., Koch, R., and Miracky, R. F.: 1980, 'Field Analysis of Magnetotelluric Data', *Abstract PM-30, Geophys.* 45, 554.
- Clarke, J., Gamble, T. D., and Goubau, W. M.: 1978, 'SQUIDs and Magnetotellurics with a Remote Reference', Invited talk to the Conference on Future Trends in Superconductive Electronics, Charlottesville, Virginia.
- Clarke, J., Goubau, W. M., and Ketchen, M. B.: 1976, 'Tunnel Junction *dc* SQUID: Fabrication, Operation, and Performance', *J. Low Temp. Phys.* 25, 94–144.
- Dawes, G.: 1980, Private communication.
- Dimitriev, V. I. and Berdichevsky, M. N.: 1979, 'The Fundamental Model of Magnetotelluric Sounding', *Proc. IEEE* 67, 1034–1044.
- Elsner, R., Kröger, P., and Micheel, H. -J.: 1982, 'Comparison of Error Analysis in Local and Reference

- Estimates of the MT Impedance Tensor', *J. Geophys./Zeit. Geophys.* (in press).
- Fischer, G.: 1980, *Ein Eindimensionales Analytisches Magnetotellurisches Umkehrverfahren*, Protokoll Kolloquium Elektromagnetische Tiefenforschung, West Berlin, pp. 231–242.
- Fischer, G., Schnegg, P. -A., Peguiron, M., and Le Quang, B. V.: 1981, 'An Analytic One-Dimensional Magnetotelluric Inversion Scheme', *Geophys. J. Roy. Astr. Soc.* **67**, 257–278.
- Fischer, G. and Schnegg, P. -A.: 1980, 'The Dispersion Relations of the Magnetotelluric Response and Their Incidence on the Inversion Problem', *Geophys. J. Roy. Astr. Soc.* **62**, 661–673.
- Gamble, T. D., Goubau, W. M., and Clarke, J.: 1979a, 'Magnetotellurics with a Remote Magnetic Reference', *Geophys.* **44**, 53–68.
- Gamble, T. D., Goubau, W. M., and Clarke, J.: 1979b, 'Error Analysis for Remote Reference Magnetotellurics', *Geophys.* **44**, 959–968.
- Goubau, W. M., Gamble, T. D., and Clarke, J.: 1978, 'Magnetotelluric Data Analysis: Removal of Bias', *Geophys.* **43**, 1157–1166.
- Harris, F. J.: 1978, 'On the Use of Windows for Harmonic Analysis with the Discrete Fourier Transform', *Proc. IEEE* **66**, 51–83.
- Hernance, J. F. and Thayer, R. E.: 1975, 'The Telluric-Magnetotelluric Method', *Geophys.* **40**, 664–668.
- Hernance, J. F., Thayer, R. E., and Björnsson, A.: 1976, *The Telluric-Magnetotelluric Method in The Regional Assessment of Geothermal Potential*, Proc. Second U.N. Symposium on the Development and Use of Geothermal Resources **2**, 1037–1048, Stock No.060–000–00005–1, Supt. Documents U.S. Government Printing Office, Washington, D.C. 20402.
- Kao, D. W. and Rankin, D.: 1977, 'Enhancement of Signal-to-Noise Ratio in Magnetotelluric Data', *Geophys.* **42**, 103–110.
- Losecke, W., Scheelke, I., and Knödel, K.: 1978, 'Magnetotellurische Tiefenerkundung in Norddeutschland', *Erdöl Kohle Erdgas Petrochem.* **31**, 23–28.
- Losecke, W., Knödel, K., and Müller, W.: 1979, 'The Conductivity Distribution in the North German Sedimentary Basin Derived from Widely Spaced Areal Magnetotelluric Measurements', *Geophys. J. Roy. Astr. Soc.* **58**, 169–179.
- Schmucker, U.: 1980, *Induktion in Geschichteten Halbräumen durch Inhomogene Felder*, Protokoll Kolloquium Elektromagnetische Tiefenforschung, West Berlin, pp. 197–210.
- Schnegg, P. -A. and Fischer, G.: 1979a, 'On-Line Determination of the Apparent Resistivities in Audio Magnetotelluric Measurements', Abstract and Oral Presentation at the 39th Annual Meeting of the German Geophys. Soc., p. 89.
- Schnegg, P. -A. and Fischer, G.: 1979b, 'On-Line Determination of the Apparent Resistivities in Audio Magnetotelluric Measurements', Abstract and Oral Presentation at the 17th IUGG General Assembly, *LAGA Bulletin* **43**, 172.
- Schnegg, P. -A. and Fischer, G.: 1980, 'On-Line Determination of the Apparent Resistivities in Audio Magnetotelluric Measurements', Protokoll Kolloquium Elektromagnetische Tiefenforschung, West Berlin, pp. 173–184.
- Schnegg, P. -A., Le Quang, B. V., and Fischer, G.: 1980, 'Management and Processing of MT Data in the Field with a Microprocessor'. Presented at the Istanbul Workshop. A written copy of their report can be obtained from the authors.
- Schumacher, P.: 1979, 'Horloges de Précision Synchronisées par l'Emetteur HBG', *Proc. Tenth Int. Congr. of Chronometry* **2**, 91–95.
- Silver, A. H. and Zimmerman, J. E.: 1967, 'Quantum States and Transitions in Weakly Connected Superconducting Rings', *Phys. Rev.* **157**, 317–340.
- Silverman, H. F.: 1977, 'An Introduction to Programming the Winograd Fourier Transform Algorithm (WFTA)', *IEEE Trans. Acoust. Speech and Sign. Process.* **ASSP-25**, 152–165.
- Sims, W. E. and Bostick, F. X. Jr.: 1969, *Methods of Magnetotelluric Analysis*, EGRL Tech. Rep. No. 58, Univ. of Texas at Austin, 86 p.
- Sims, W. E., Bostick, F. X. Jr., and Smith, H. W.: 1971, 'The Estimation of Magnetotelluric Impedance Tensor Elements from Measured Data', *Geophys.* **36**, 938–942.
- Solyman, L.: 1972, *Superconductive Tunnelling and Applications*, Chapman and Hall, London, 406 + XII pages.
- Stanley, W. D., Boehl, J. E., Bostick, F. X., and Smith, H. W.: 1977, 'Geothermal Significance of Magnetotelluric Sounding in the Eastern Snake River Plain – Yellowstone Region', *J. Geophys. Res.*

82, 2501–2514.

Thayer, R. E., Björnsson, A., Alvarez, L., and Hermance, J. F.: 1981, 'Magma Genesis and Crustal Spreading in the Northern Neovolcanic Zone of Iceland: Telluric-Magnetotelluric Constraints', *Geophys. J. Roy. Astr. Soc.* **65**, 423–442.

Voss, R. F., Laibowitz, R. B., Raider, S. I., and Clarke, J.: 1980, 'Al-Nb Low Noise dc-SQUID with 1 μm Tunnel Junctions', *J. Appl. Phys.* **51**, 2306–2309.

Vozoff, K.: 1980a, 'Electromagnetic Methods in Applied Geophysics', *Geophys. Surveys* **4**, 9–29.

Vozoff, K.: 1980b, 'Report on an Informal Workshop on Natural EM Fields at Audio Frequencies. Held under the Auspices of IAGA at the 1979 Assembly, Canberra', *IAGA News* **18**, 92–93.

Weidelt, P.: 1972, 'The Inverse Problem of Geomagnetic Induction', *J. Geophys./Z. Geophys.* **38**, 257–289.